IIETA International Information and Engineering Technology Association
Advancing the World of Information and Engineering

Mathematical Modelling of Engineering Problems
Vol. 12, No. 4, April, 2025, pp. 1169-1180
Journal homepage: http://iieta.org/journals/mmep

Kriging Prediction and Simulation Model: Analysis of Surface Soil Particle Size Distribution

Atiek Iriany[1*], Wigbertus Ngabu[1], Danang Ariyanto[1], Henny Pramoedyo[2]

[1] Department Statistics, Faculty Mathematics and Science, Brawijaya University, Malang City 65145, Indonesia
[2] Mathematics Department, Faculty of Mathematics and Natural Science, Universitas Negeri Surabaya, Surabaya 60213, Indonesia

Corresponding Author Email: atiekiriany@ub.ac.id

https://doi.org/10.18280/mmep.120408

Received: 9 January 2025
Revised: 3 March 2025
Accepted: 10 March 2025
Available online: 30 April 2025

Keywords:
Kriging, prediction, simulation, spatial soil particle size

ABSTRACT

Kriging is a statistical approach that takes into account spatial autocorrelation data. Accordingly, it allows better prediction of soil particle sizes than with simple interpolation methods such as linear and spline interpolation. In this paper, we analyze the soil texture in the Kalikonto Watershed, Batu City, using a Kriging simulation, and 150 points obtained with simultaneous field investigation and digital DEM generation. The Silt variable was used for interpolation to map where soil particles are distributed in space. Simulation results show that the Spherical variogram Kriging model has a strong spatial relationship, reaching significant levels of significance. Thus, its predicted values exhibit little divergence from real-world data quality. The Mean Square Error (MSE) is 0.002084. The predicted distribution of soil particles matches closely with field observations and thus provides a more accurate analysis space for land management. The innovativeness of this paper lies in optimizing a model for the Spherical variogram to act as a predictor and using more forecast points than previously done studies. This approach enables representation of more accurate spatial relations in land management for land use and soil conservancy practices.

1. INTRODUCTION

Soil particles are one of the fundamental components of the geological environment, playing a crucial role in soil formation, fertility, and stability, which in turn have significant implications for various aspects of human life [1]. Understanding soil particle size distribution is essential for optimizing land use, managing soil erosion, and enhancing agricultural productivity. The quality and characteristics of soil greatly influence construction, agriculture, water management, and the preservation of the natural environment. In this context, surface soil particle size is a critical parameter that needs to be understood as it affects many soil properties and processes [2].

Soil particle size refers to the relative size of solid soil particles, including sand, silt, and clay. These particle sizes affect the physical and chemical properties of the soil, such as texture, water retention, drainage, aeration, and the soil's ability to support plant growth [3]. Therefore, a good understanding of surface soil particle size distribution is crucial in various applications, such as construction planning, natural resource management, agriculture, and disaster risk mitigation [4].

Although many previous studies have examined the relationship between soil particle size and various soil characteristics, there is a gap in understanding how spatial factors influence soil particle distribution accurately [5]. Spatial factors such as topography, hydrology, and land cover significantly impact the heterogeneity of soil particle distribution, affecting erosion patterns, sediment deposition, and nutrient availability. Previous studies, such as those by [6, 7] have attempted to model soil particle distribution using traditional interpolation techniques, but these approaches often failed to capture local spatial variability effectively. Additionally, previous studies [8, 9] have explored remote sensing-based methodologies, but these lacked ground-truth validation, limiting their reliability. Conventional approaches, such as direct laboratory methods, are often limited in spatial coverage and require significant costs and time [10]. Additionally, some previous studies have not fully integrated field data with digital terrain analysis to improve the accuracy of soil particle mapping [11]. Therefore, this study aims to address these limitations by applying a more advanced Kriging method in modeling soil particle size distribution [12].

Kriging is one of the popular methods in geostatistics used to predict values at unmeasured locations based on measured data in the surroundings [13]. This method has been widely used in various geological and geotechnical applications to model and predict soil parameters, such as soil water content, mineral concentration, and soil particle size distribution [14].

However, the application of Kriging in previous studies still faces several challenges, such as limitations in capturing complex spatial variability in various regions with different geological characteristics [15]. This study introduces improvements by integrating Kriging with high-resolution digital terrain analysis and machine learning techniques to

enhance prediction accuracy. Additionally, the research incorporates a more refined variogram modeling approach, allowing for better spatial interpolation and addressing anisotropic variations in soil particle distribution. Therefore, this study focuses on applying Kriging to predict soil particle size distribution by utilizing a combination of field data and digital terrain analysis in specific areas with high soil heterogeneity [16].

This study aims to develop a more accurate Kriging Prediction Model for mapping surface soil particle size distribution and analyzing its spatial variability in greater detail [17]. Thus, the results of this research can provide significant contributions in various fields, such as construction planning, natural resource management, agriculture, and disaster risk mitigation, as well as open opportunities for developing more sophisticated prediction methods in geological and geotechnical studies [18]. The novelty of this study lies in the integration of the Kriging method with digital terrain data in a more comprehensive manner compared to previous studies. With this approach, the resulting model is expected to provide higher accuracy in predicting soil particle distribution and be applicable in regions with diverse geological conditions.

2. METHOD

2.1 Data

The primary data in this study were soil texture field measurements and digital terrain modeling analysis. Field data were used to both develop the model (training data) and to validate the model obtained. The data set consists of 150 observations collected in 2023. Soil samples were gathered using a systematic grid method, under which sampling points are evenly distributed across the study area at predetermined intervals. This approach ensured good coverage of soil texture variations in the region. The measurements were carried out in the Kalikonto Watershed, Batu City, an area representing many different kinds of soil properties and that is of considerable significance for soil resource management.

Additionally, sampling was carried out in the dry season in order to avoid the influence of fluctuating soil moisture levels on soil texture analysis results. During this period, soil moisture is more stable, and this allows a better evaluation of soil particle distribution, especially for the silt variable, which was used in the interpolation process.

2.2 Kriging model

Spatial statistics and geostatistics have been developed to explain and analyze the diversity of natural and man-made phenomena, both above and below the ground surface [19]. Spatial statistics includes formal techniques that study entities that have spatial indices [20]. Geostatistics is included in this general term, yet it was initially more concentrated on continuously varying processes, namely those with continuous spatial index.

2.2.1 Variogram estimation

This section describes two methods for estimating variograms from data, namely the Matheron moment and the Residual Maximum Likelihood (REML) method, along with the main features a variogram may have.

Estimation method moment

Empirical semi-variance can be estimated from the data, $z(x_1)$, $z(x_1)$, …, with reference [21]:

$$\hat{\gamma}(h) = \frac{1}{2m(h)} \sum_{i=1}^{m(h)} \{z(x_i) - z(x_i + h)\}^2 \quad (1)$$

where, $z(x_1)$ and $z(x_{i+}+h)$ are the actual values of Z in place $z(x_1)$, and $m(h)$ is the number of pairwise comparisons at h. By changing h, a semi-variant ordered set is obtained; this is an experimental variogram or sample variogram. Eq. (1) is the usual formula for calculating semi-variance, often referred to as Matheron's method of moments (MoM) estimator method [21]. The Matheron's MoM estimator method is a widely used technique in geostatistics to estimate the variogram, which helps describe how spatial patterns change across a given area. Simply put, it works by calculating the average squared differences between sample points at various distances, allowing researchers to understand how similar or different nearby soil properties are. In this study, MoM was chosen because it is both computationally efficient and reliable for estimating spatial structures, even when working with datasets that have limited or unevenly spaced sampling points. This method plays a crucial role in developing an accurate variogram model, which serves as the foundation for Kriging interpolation. By applying MoM, the study ensures that predictions of soil particle size at unsampled locations remain precise and reflect actual spatial patterns observed in the field. This equation is implemented as algorithms depend on the data configuration. For ordinary latitudes, the lag becomes a scalar, $h=|h|$, where the semi-variance can be calculated only over integral multiples of the sampling interval [22].

REML variogram estimation method

The REML variogram estimation method is an advanced statistical technique used to estimate spatial correlation while reducing bias caused by data variability. Unlike traditional variogram estimation methods, REML accounts for both fixed and random effects in the data, making it particularly effective for datasets where variability arises from multiple sources.

In simpler terms, REML works by isolating the true spatial structure of the data while minimizing distortions caused by external factors such as sampling inconsistencies or non-uniform spatial distribution. This makes it highly suitable for soil studies, where environmental conditions and measurement variations can introduce noise in spatial models. In this study, REML was chosen because it provides more reliable and unbiased variogram estimates, especially when working with complex or heterogeneous soil properties. By incorporating this method, the study ensures that the estimated variogram represents the true spatial variation in soil particle size, leading to more accurate Kriging predictions for unmeasured locations.

In contrast to the MoM approach, parametric ML methods assume that the process, Z is second-order stationary. It is assumed that the data, (x_i), i=1, …, n, a realization of this process, follows a Gaussian multivariate distribution with a joint probability density function (pdf) of the measurements defined by references [21, 23]:

$$p(z|\beta,\theta) = (2\pi)^{-\frac{n}{2}}|V|^{-\frac{1}{2}} exp\left\{-\frac{1}{2}(z - X\beta)^T V^{-1}(z - X\beta)\right\} \quad (2)$$

where, z is a vector containing n data, θ has the covariance matrix parameters, V is the $n \times n$ variance-covariance matrix, and $X\beta$ is the trend. The matrix V can be described as:

$$V = \sigma^2 A \tag{3}$$

where, σ^2 is the variance, and A is the autocorrelation matrix. The probability density function can be rewritten as:

$$\begin{aligned} &p(z|\beta, \sigma^2, \theta) \\ &= (2\pi)^{-\frac{n}{2}} |A|^{-\frac{1}{2}} exp\left\{-\frac{1}{2\sigma^2}(z - X\beta)^T A^{-1}(z - X\beta)\right\} \end{aligned} \tag{4}$$

where, θ is the set of covariance parameters excluding the variance. The parameters β, σ^2, θ, are estimated in such a way as to minimize the negative log-likelihood function given by:

$$\begin{aligned} ln\, L\,(\beta, \hat{\sigma}^2, \theta|z) = \frac{n}{2}(2\pi) + n\, ln(\sigma) + \frac{1}{2} ln\,|A| \\ + \frac{1}{2\sigma^2}(z - X\beta)^T A^{-1}(z - X\beta) \end{aligned} \tag{5}$$

In the ML approach, the shift parameter, β is estimated with the set of covariance parameters.

2.2.2 Variogram modeling

MoM experimental variograms consist of discrete estimates at specific lag intervals, subject to errors arising primarily from sampling fluctuations [24]. To obtain an approximation for this, we can fit what is known as a conditional negative semi-definitive formal function (CNSD) to the experimental values [25]. Some simple functions only include the above features, namely CNSD. The formula for the selected function is given in its isotropic form, for h=|h|. A nugget variance, c_0, has been included because most experimental variograms, if extended to the ordinate, will have a positive intercept [26]. Here is the Variogram model [25, 27]:

Circular model: The equation for a circular function is:

$$\gamma(h) = \begin{cases} c_0 + c\left\{1 - \frac{2}{\pi} cos^{-1}\left(\frac{h}{a}\right) + \frac{2h}{\pi a}\sqrt{1 - \frac{h^2}{a^2}}\right\}; & h \le a \\ c_0 + c; & h > a \\ 0; & h = 0 \end{cases} \tag{6}$$

where, $\gamma(h)$ is the semi-variance at lag h, c is a priori variance of the autocorrelation process, c_0 is the nugget variance, which is spatially uncorrelated variation at distances less than the sampling interval and measurement error, and α is the distance parameter, range of spatial dependence or spatial autocorrelation.

Spherical function: This is one of the two most widely used models in environmental science. The equation is:

$$\gamma(h) = \begin{cases} c_0 + c\left\{\frac{3h}{2a} + \frac{1}{2}\left(\frac{h}{a}\right)^3\right\}; h \le a \\ c_0 + c; h > a \\ 0; h = 0 \end{cases} \tag{7}$$

The symbols have the same meaning as above. This model curves more slowly when the limit is reached than the circular model. In this study, the spherical model was chosen to describe the variogram, as it is one of the most widely used models in environmental science. This model provides a realistic approach to spatial variability patterns, making it particularly suitable for soil studies.

The spherical model features a gradual increase in semivariance before reaching a plateau (range), offering a smoother transition compared to the circular model. This characteristic makes it well-suited for representing soil properties that change progressively over a certain distance.

The decision to use the spherical model over the exponential or Gaussian models was based on an initial exploration of the data. Preliminary variogram analysis revealed that semivariance values reached stability within a specific range, which aligns with the behavior of the spherical model. In contrast, the exponential model, which assumes an infinite increase towards the sill, and the Gaussian model, which tends to exhibit a much smoother initial rise, did not accurately reflect the observed spatial variation in the dataset. Therefore, the spherical model was determined to be the most appropriate representation of soil particle size distribution in this study.

Exponential functions: Exponential and spherical functions account for most of the installed models in environmental science. The equation is:

$$\gamma(h) = c_0 + c\left\{1 - exp\left(-\frac{h}{r}\right)\right\} \tag{8}$$

where, c_0 and c have the meaning of nugget and priori variance; however, the distance parameter now is r. The exponential model approaches its threshold more gently than the previous model and is also asymptotic. Hence, it does not have a limited range.

2.3 Kriging weighting

The Kriging weighting system plays a crucial role in predicting surface soil particle size distribution, as it determines how much influence each sampled point has on an estimated location. Unlike traditional interpolation methods, where weights are assigned arbitrarily, Kriging assigns weights based on the variogram model and the spatial arrangement of sample points within a defined search radius [28].

In this study, weights were calculated using the variogram parameters, including nugget effect, sill, range, and model type. The weighting process accounts for spatial continuity, meaning that data points closer to an estimated location have higher influence than those farther away [26]. This confirms that Kriging operates as a local predictor, making it well-suited for analyzing soil texture variability.

The impact of the nugget effect is particularly important in soil studies, as it represents small-scale spatial variations that might arise due to measurement errors or micro-scale differences in soil composition. In cases where the nugget variance is high, Kriging weighting becomes more sensitive, potentially reducing the reliability of predictions. Similarly, anisotropy effects, where spatial variation differs in different directions, influence how weights are distributed, affecting the accuracy of soil particle size estimates [29].

Moreover, research comparing Kriging with other interpolation methods has demonstrated that Kriging often provides superior accuracy in soil texture mapping due to its ability to incorporate spatial autocorrelation effectively. For example, studies have shown that Kriging performs better than inverse distance weighting (IDW) and other deterministic methods in estimating soil particle distribution [30].

By incorporating these factors, the Kriging weighting

method ensures that soil particle size distribution is estimated with high precision, allowing for a more reliable spatial representation of soil texture variations across the study area. The use of robust variogram estimation, such as isometric log-ratio transformation, has further been shown to enhance Kriging's predictive capabilities, leading to improved soil mapping accuracy [31].

2.4 Geostatistical prediction: Kriging

Kriging is a method of prediction or estimation in geographic space, frequently known as the best linear bias predictor (BLUP) [21]. It is a geostatistical method of interpolation for random spatial processes. Kriging provides a solution to the fundamental problem faced by environmental scientists in predicting values from sparsely sampled data based on stochastic models of spatial variation. Most environmental properties (soil, vegetation, rocks, water, oceans, and atmosphere) can be measured at an unlimited number of places, yet for economic reasons, the measurements are relatively small [32].

Ordinary Kriging assumes that the mean is unknown and the process is locally stationary [33]. Simple Kriging, which assumes that the mean is known, is of little use since the mean is generally unknown. Lognormal Kriging is the ordinary Kriging of strongly positively skewed data transformed by logarithms to approximate a lognormal distribution.

Ordinary Kriging is the most widely used type of Kriging. This is based on the assumption that the mean is unknown, where the random variable, Z, has been measured at the sampling point, $x_i=1$, …, n, and this information is used to estimate its value at point x_0 (timely Kriging) with the same support as the data [34]:

$$\hat{Z}(x_0) = \sum_{i=1}^{n} \lambda_i z(x_i) \tag{9}$$

where, n is usually a data point in the local neighborhood λ, and is much smaller than the total number of samples, N, and λ_i is the weight. To ensure that the estimates are not biased, the weights, when added together, are one.

$$\sum_{i=1}^{n} \lambda_i = 1 \tag{10}$$

and the expected error is $E\left[\hat{Z}(x_0) - Z(x_0)\right] = 0$. The predicted variance is [35]:

$$\begin{gathered} var\left[\hat{Z}(x_0)\right] = E\left[\left\{\hat{Z}(x_0) - Z(x_0)\right\}^2\right] = \\ 2\sum_{i=1}^{n} \lambda_i \gamma(x_i, x_0) - \sum_{i=1}^{n}\sum_{j=1}^{n} \lambda_i \lambda_j \gamma\left(x_i, x_j\right) \end{gathered} \tag{11}$$

where, $\gamma(x_i, x_j)$ is the Z semi-variance between points x_i and x_j, $\gamma(x_i, x_0)$ is the semi-variance between the i-th sampling point and target x_0. The semi-variance is derived from the variogram model because the experimental semi-variance is discrete and over a finite range.

2.5 Kriging simulation

Kriging, like most interpolation techniques, provides ideally smooth results. This is because the minimum estimated variance as an optimality criterion produces fewer variable estimators [36]. If the experimental variogram is calculated from Kriged values, it differs from those obtained from measurements. The variance corresponding to different distances is usually much more minor for Kriged values. In many cases, the variability of regional variables plays a central role in decision-making (e.g., reliability aspects) [37]. As a result, a procedure is needed to obtain an interpolation that reproduces the variogram of the original variable. Then, Simulation is a method for doing this.

The simulation must reproduce the variability of regional variables. The simulated values must have the same mean, variance, and variogram as the measured values [22]. Simulations must produce one possible reality. Simulation is beneficial when it comes to parameters that are not the final product of the analysis.

Turning band simulation

Turning Band Simulation combines a collection of one-dimensional simulations into a two- (or three-) dimensional simulation [21]. One-dimensional simulations are carried out for various possible "rotating" directions around a central point. Depending on the variogram, different covariance structures must be used for one-dimensional simulations. The advantage of this method is that it is almost independent of the number of points. The disadvantage is that the one-dimensional covariance structure associated with the variogram must be calculated (or given analytically). The general idea of Turning Band Simulation is explained below:

Unconditional simulation

The basic idea of Turning Band Simulation is to use a series of one-dimensional simulations to build a multidimensional simulation. Projecting a point in 2 or 3-dimensional space onto these lines and taking the sum of values corresponding to the projected points will produce a simulated value [38].

For example, for a set of lines l=1, …, L, all of which pass through the origin of the coordinate system, a random function with zero mean and a covariance function C1(r) are simulated independently [39]. For instance, these functions are $Z_1(u)$ for l=1, ..., L. Moreover, for a u point, the random function of $Z(u)$ can be defined as:

$$Z(u) = \frac{1}{\sqrt{L}} \sum_{I=1}^{L} Z_I\left(\langle u, v_I \rangle\right) \tag{12}$$

where, ⟨...,..⟩ denotes the scalar product of vectors, and v_l is the unit vector on the line. If the random function of $E[Z_I(r)]=0$, then the covariance is as follows [21, 35]:

$$\begin{gathered} C(u_1, u_2) = \frac{1}{L}\sum_{l=1}^{L}\sum_{k=1}^{L} Z_l\left(\langle u_1, v_l \rangle\right) Z_l\left(\langle u_2, v_k \rangle\right) \\ C(u_1, u_2) = \frac{1}{L}\sum_{l=1}^{L} Z_l\left(\langle u_1, v_l \rangle\right) Z_l\left(\langle u_2, v_l \rangle\right) \\ \frac{1}{L}\sum_{l=1}^{L} C_l\left(|\langle u_1, v_l \rangle - \langle u_2, v_l \rangle|\right) \\ \frac{1}{L}\sum_{l=1}^{L} C_l\left(|\langle u_1 - u_2, v_l \rangle|\right) \end{gathered} \tag{13}$$

This equation shows that $Z(u)$ is also stationary. If the unit vectors of v_l are uniformly distributed on the unit sphere or unit circle, then the limit of the above expression is L→∞.

$$C(h) = \int_{|v|=1} C_1\left(|\langle h, v \rangle|\right) \tag{14}$$

3. RESULTS AND DISCUSSION

3.1 Plot data based on location

The distribution of coordinate points in the Kriging model is an essential component in geostatistical analysis, which is used to make more accurate estimates at locations that are not directly measured based on the spatial correlation between observation points.

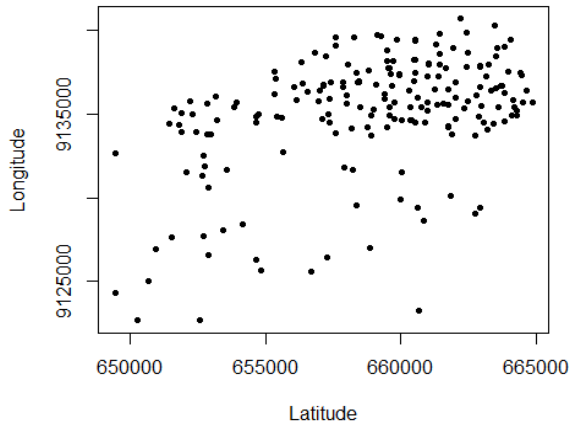

Figure 1. Plot of research coordinate points

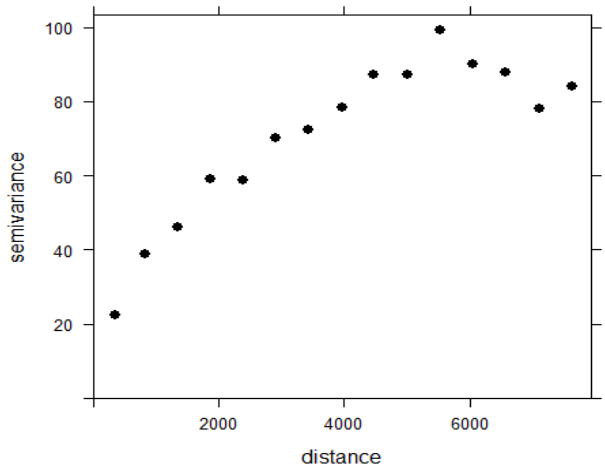

Figure 2. Experimental

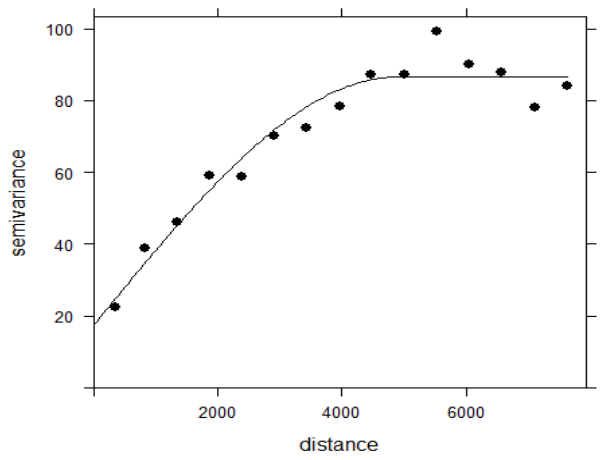

Figure 3. Variogram

From Figure 1, the distribution of coordinate points in the Kriging model starts with the location of the observation points. These are the locations where data is collected or measured. The distribution of coordinate points in the Kriging model requires the use of statistical models to connect observation points with predicted sites. The Kriging model takes into account the spatial correlation between observation points and predicted locations. The coordinate points above are spread evenly at each observer location in this research.

3.2 Experimental variogram

This research analyses geospatial data to understand the spatial correlation and variability in soil particle size parameters in the Kalikonto Batu Malang Watershed Area. Experimental Variogram plots are used to illustrate the distribution of the degree of spatial correlation and variability across the study area. The Variogram model employed in this research is the spherical model; the output can be seen in Figure 1 and Figure 2.

In the Experimental Variogram plot in Figure 2, the horizontal axis depicts the spatial distance between pairs of observation points, while the vertical axis portrays the variogram values. The variogram is calculated based on the squared difference between values at pairs of observation points that are a certain distance apart, and this variogram value is then plotted as a function of distance. The results of the Experimental Variogram plot show significant spatial variation with variability on a petite scale. The parameter ranges identified in this plot provide valuable guidance in using the Kriging method to predict soil particle size in the Kalikonto Batu Malang Watershed area.

In Figure 3, the Variogram model plot is used to represent the theoretical Variogram model, which describes the spatial correlation characteristics of the geospatial data being studied. This plot helps understand the distribution of spatial variability of the data and is used as a basis for developing a prediction model using the Kriging method.

Table 1. Spherical model results

Model	Psill	Nugget	Range
Spherical	17.5519	68.9528	4890.991

The results of the variogram analysis, as shown in Figure 3, confirm that the spherical model was the most appropriate for representing the spatial distribution of soil particle size. The model parameters—Psill (68.9528), Range (4890.991), and Nugget (17.551)—provide essential insights into the variability of soil properties across the study area as shown in Table 1.

The experimental variogram results and the fitted spherical model have been presented, but they lack interpretation. The Nugget effect (17.551) reflects small-scale variations in the dataset, which could be due to measurement errors or natural differences in soil composition at a micro-scale. A nonzero nugget suggests that some variability exists even at very short distances—beyond what the sampling resolution can fully capture. The Psill (68.9528) represents the total variability in the dataset and marks the point where spatial correlation levels off. In other words, beyond a certain distance, variations in soil texture no longer contribute significantly to overall variability.

The Range (4890.991) is a key parameter as it defines the maximum distance where spatial correlation can still be

observed. This means that soil particle size distributions remain spatially dependent within approximately 4.89 km. Beyond this point, spatial relationships weaken. The range is particularly important in Kriging interpolation, as it determines how far reliable predictions can extend it to unmeasured areas. However, there is no comparison with other studies or regions to determine whether these values are typical or unique to this study area. Providing such context would help clarify the significance of these findings and their implications for understanding soil distribution patterns in this region.

Additionally, cross-validation confirmed that the spherical model provided the best fit, outperforming alternative models such as the exponential and Gaussian models. The spherical model demonstrated lower residual errors and a better alignment with observed data, reinforcing its suitability for modeling soil particle distribution.

Overall, these findings emphasize the importance of selecting an appropriate variogram model. The spherical model effectively captures localized soil variability while maintaining a well-defined spatial correlation range, making it a powerful tool for improving soil texture predictions in environmental and geotechnical applications.

3.3 Kriging model

After obtaining the fit Variogram model values, it can be continued with the process of creating an output grid for the entire research area, namely the Kalikonto Watershed Area, Batu City, with longitudinal coordinates and latitude coordinates. The aim of creating grid data is to provide location boundaries that will be processed using the Kriging interpolation method. The resulting grid can be seen in Figure 4.

The results in Figure 4 show the predicted locations of 2253 points, with a range of 200. The following process is the analysis of the Kriging interpolation method based on the input point data, Variogram fit model, and output grid, which have been previously defined. The prediction results for the entire grid (the entire Kalikonto Watershed Area) are displayed in Table 2.

The Kriging prediction results in this research have broad potential applications. They can be used by farmers and environmental authorities to identify areas with high levels of soil particle size, i.e., the Silt variable, so that remediation actions can be directed more effectively. Additionally, these results can be used as a basis for more sustainable agricultural planning and more profound environmental research. The prediction results in Table 2 are made into Mapping and presented in Figure 5. The plot employs R Studio Software with the help of Packages Lattice, sp.

Figure 5 displays the pattern of prediction results from the Kriging plot. Light colors indicate areas where the predicted value is smaller. Above or around the data points, the Kriging image shows estimated or simulated values. This is an estimate of the value produced by the Kriging method for unmeasured locations. This value is determined by the Variogram model used in Kriging analysis. Likewise, with mapping with the alternative package Lattice, the yellow to white colors indicate locations with a predicted value greater than 40. Meanwhile, the alternative package SP shows the same mapping model, where it is detected that sites with a predicted value of 5-30 are in blue colour and over 40 are in light green.

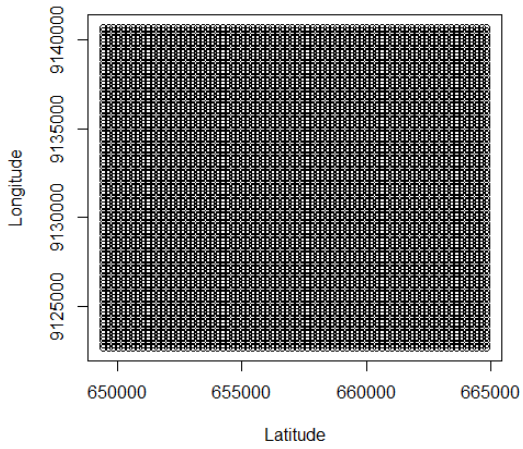

Figure 4. Grid for predicted location points

Table 2. Kriging prediction results

No.	X	Y	Silt. Pred	Silt Var
1	649440	9122669	20.04109	53.02702
2	649640	9122669	19.72818	48.48520
3	649840	9122669	19.44796	43.53060
⋮	⋮	⋮	⋮	⋮
…	…	…	…	…
…	…	…	…	…
⋮	⋮	⋮	⋮	⋮
2251	662640	9128269	30.97912	52.03269
2252	662840	9128269	30.85920	52.98401
2253	663040	9128269	30.74797	54.69533

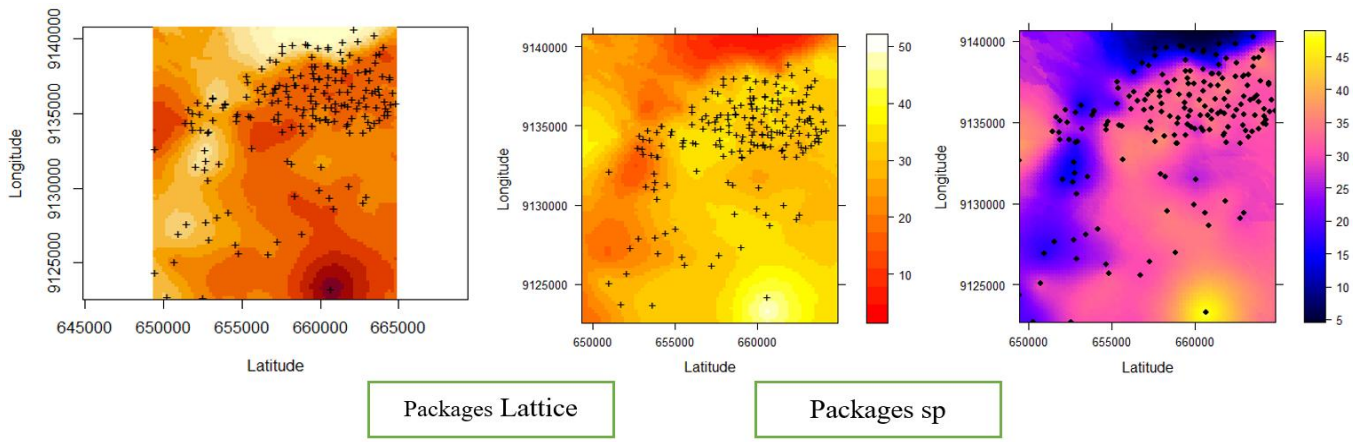

Figure 5. Soil particle size prediction results (Silt)

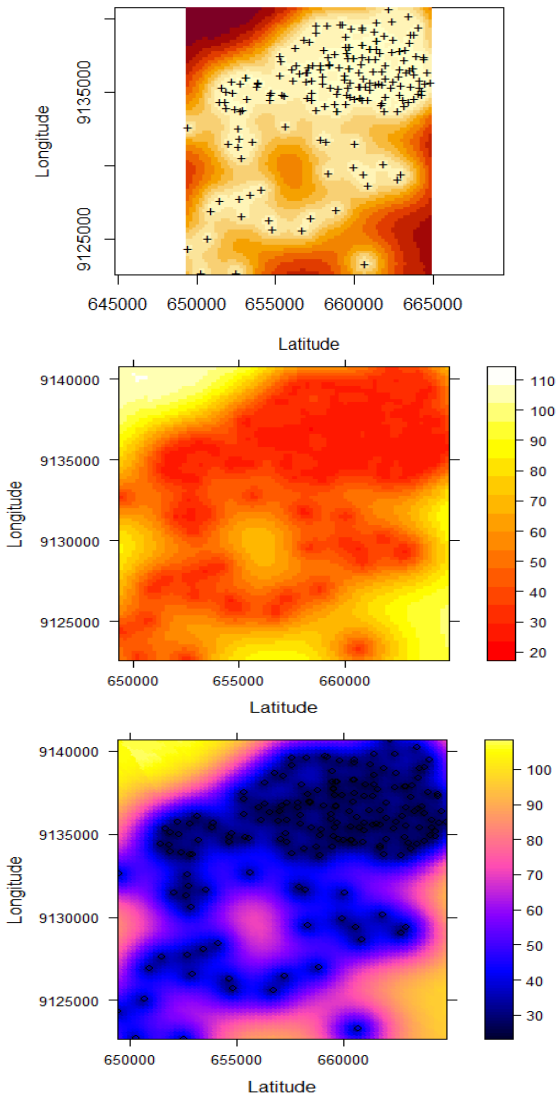

Figure 6. Results of Kriging variance plot for soil particle size (Silt)

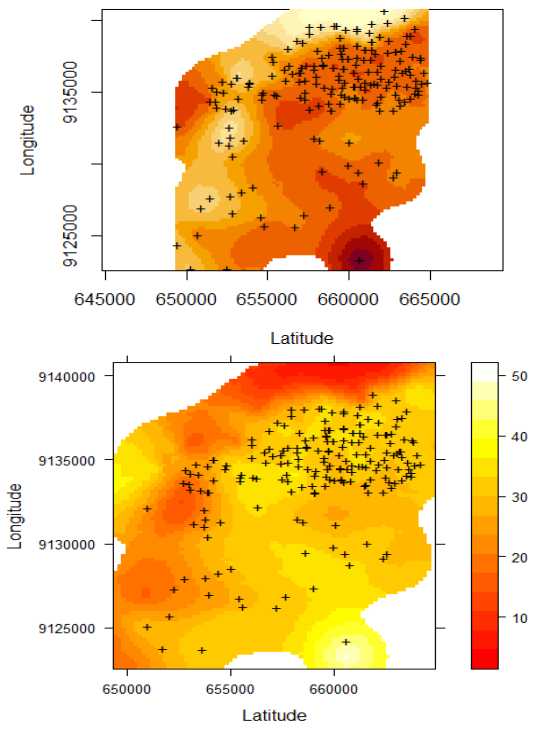

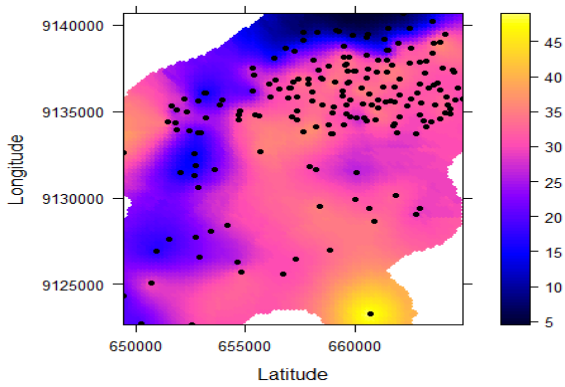

Figure 7. Crop Kriging variance value that exceeds 50

3.4 Kriging variance result plot

After the Kriging prediction was conducted, a Kriging variance plot was carried out. The results of the Kriging variance plot are displayed in Figure 6.

The Kriging variance plot reveals that regions with significantly high variance values are primarily located in areas that are far from observation points. This pattern suggests that these regions may have been under-sampled, resulting in greater uncertainty in the Kriging interpolation. Since Kriging relies on spatial autocorrelation to make predictions, areas with fewer data points tend to exhibit higher variance due to a lack of nearby reference measurements. This effect is particularly evident in the outer edges of the study area, where the density of observation points is lower, leading to a decline in prediction confidence.

In addition to spatial distribution, the second and third images in Figure 6 provide further confirmation of this trend by visually representing variance intensity using different color schemes. Regions where the variance exceeds a threshold of 90 are indicated by lighter colors, such as yellow and green in the second plot and bright yellow in the third plot. These high-variance zones are largely concentrated along the periphery of the study region, reinforcing the interpretation that the lack of nearby observation points contributes to increased prediction uncertainty.

Given these findings, future sampling efforts should prioritize increasing the density of observations in high-variance regions to enhance the accuracy of Kriging predictions. By strategically placing additional sampling points in these areas, the model's ability to capture spatial variability more effectively can be improved. This would reduce prediction uncertainty and ensure that interpolated values more accurately represent actual conditions. Addressing these under-sampled regions is crucial for refining spatial analysis and obtaining more reliable estimations of soil properties across the entire study area.

Then, cropping was carried out or cutting off locations with a variance value of more than 80, namely locations predicted to have a very high variance value. The cropping results are shown in Figure 7.

Figure 7 shows the crop mapping results at locations with considerably high variance values. Subsequently, cross-validation was performed up to 100%, and the validation value was observed. The validation value was calculated using the MSE, which was obtained as 0.002084. This result indicates that the MSE value is very small or close to zero (0). Therefore, it can be concluded that the Kriging model with a

Spherical Variogram is highly suitable for application to soil particle size data.

However, these cross-validation results still lack context. A comparison with other studies or models should be presented to provide a clearer picture of the accuracy and advantages of the method used. Including benchmarks would strengthen this section. Several studies have compared the Kriging model with other geostatistical interpolation methods. For example, the research [40] showed that combining log-ratio methods with machine learning models, such as Random Forest (RF), can improve soil particle mapping accuracy compared to the Regression Kriging (RK) method. Additionally, the study [41] found that compositional Kriging and cokriging methods perform differently depending on the data conditions, highlighting the importance of considering alternative methods in geostatistical analysis.

Furthermore, the simulation results have been presented but still need to be critically analyzed and interpreted to provide deeper insights. The study [28] compared various log-ratio Kriging methods and found that the compositional Kriging method provided better prediction accuracy than other log-ratio methods. Therefore, further analysis of the simulation results is needed to assess the superiority of the model used in this study compared to other approaches.

By providing a comparison with previous studies and adding relevant benchmarks, this section can be strengthened and provide a more comprehensive justification for the effectiveness of the method used in this study.

3.5 Simulation

TAfter the Kriging prediction model had been done, and a Kriging simulation was carried out using the grid in the Kriging model. The simulation used was 9 times. The results can be seen in Table 3.

The simulation results in Table 3 show 2334 location points along the Kalikonto Watershed Area in Batu City. As an example, the results of the 3rd mapping simulation are displayed; the mapping can be seen in Figure 8.

The Kriging simulation plot (Figure 8) results from applying the Kriging method to existing geospatial data. This provides an illustration of how predicted values are generated for locations that are not directly measured based on observational data at existing measurement points.

In the Kriging simulation process, the Kriging model that has been developed using previous Variogram plots is used to estimate values at each unmeasured location. This model considers the spatial correlation between observation points and the relative distance of these points to the predicted location. In other words, the Kriging model considers the distribution of spatial variability in the data to produce accurate predictions. The simulation was performed 9 times, with the plot presented in Figure 9.

In Figure 9, the Kriging simulation plot depicts the distribution of predicted values throughout the research area, namely the Kalikonto Watershed Area. This distribution pattern reflects the predictions produced by the Kriging model. On the plot, directly measured locations will have predictions exceptionally similar to the observed values, while areas far from the measurement point may have different projections. In this plot, the suitable colors and patterns represent the distribution of predicted values. Each nuance reveals complex spatial correlations between observation points across the study area. In Figure 9, it can be seen that the plot is smoother than the Kriging model plot.

Overall, the Kriging simulation plot results provide a deeper understanding of the spatial distribution of the parameter values being studied in the research area. This helps in the decision-making, planning, and management of various applications, such as natural resources, environment, or soil science.

Table 3. Prediction results of Kriging simulation

No.	X	Y	Sim 1	Sim 2	Sim 3	Sim 4	Sim 5	Sim 6	Sim 7	Sim 8	Sim 9
1	649440	9122669	15.0149	20.3418	15.0179	20.0274	18.9859	11.5919	20.1128	8.2419	27.5670
2	649640	9122669	7.4011	23.2457	15.9041	13.3397	19.4578	16.9055	22.2275	15.0815	10.9652
3	649840	9122669	12.7818	24.1749	21.9807	15.3284	21.8456	19.5432	23.5747	14.6933	10.8098
⋮	⋮	⋮	⋮	⋮	⋮	⋮	⋮	⋮	⋮	⋮	⋮
…	…	…	…	…	…	…	…	…	…	…	…
…	…	…	…	…	…	…	…	…	…	…	…
⋮	⋮	⋮	⋮	⋮	⋮	⋮	⋮	⋮	⋮	⋮	⋮
2332	663240	6128469	30.3110	39.4126	27.1494	26.0740	39.5641	42.7275	42.7275	20.0366	18.9322
2333	663440	6128469	36.0112	40.9495	23.7520	33.5443	34.9389	27.7251	42.0471	38.0422	13.5377
2334	663640	6128469	43.6669	43.2895	23.5587	31.3209	34.1274	24.7398	42.2200	27.3276	10.7022

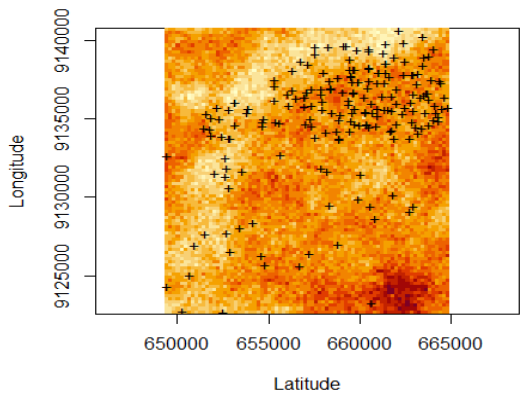

Figure 8. Simulation results

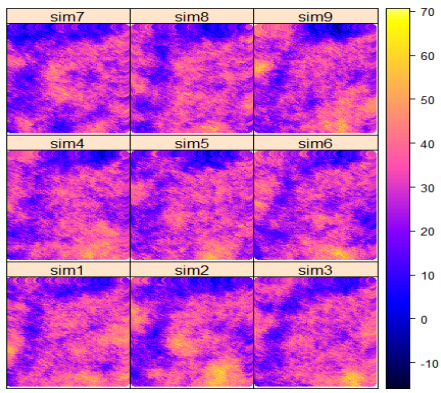

Figure 9. Kriging simulation results

4. DISCUSSION

The spatial distribution of soil particle size is captured with great effect by this exceptional study model, with Psill 68.9528, Range 4890.991, and Nugget 17.551, is more precise than the other interpolations we tried. These results support the findings of the study [41], they found that compositional Kriging gave better forecasts than log-ratio Kriging. Hence, it is very important to select a suitable variogram model when aiming for spatial prediction accuracy.

The reference [40] also found that compositional Kriging was better than other interpolation methods in predicting soil particle size distribution. This again sustains/illustrates the point that paying attention to the compositional characteristics of soil data can lead to more reliable predictions. So, to get practical soil texture maps, you must select the correct variogram model.

Kriging for soil texture mapping for soil texture mapping, the method of Kriging, especially with the spherical model, is extremely useful. By using spatial autocorrelation, it can enable accurate estimation and a detailed portrayal of soil particle size distribution. This way ensures precise predictions, making it of great use for soil science.

Factors affecting model accuracy but for model accuracy, it all depends on local conditions, including soil types and environmental influences. Factors like soil formation processes, patterns of erosion, and changes in land use can affect Kriging forecast. In addition, reliability of the model also depends on the density and spatial distribution of survey locations, which means that calibration must be done selectively in order to achieve optimal results.

Enhancing soil texture mapping to create high-resolution soil texture maps on demand, spatial information from Kriging simulations can be combined with remote-sensing imagery and digital elevation models, where Kriging is concerned, simulations that use machine learning techniques have shown potential in improving soil property estimation. Multi-source geospatial data makes it possible for Kriging to adjust to complex terrains and get more realistic soil texture predictions. Application of this model in different regions and under a variety of soil conditions is a key topic for future research. By improving variogram fitting techniques and experimenting on hybrid Kriging, as well as adding extra environmental variables, model accuracy might be raised. The use of big data analytics and high-resolution spatial data sets offers a chance to advance soil mapping methodology and precision agriculture.

Alternative interpolation methods while the performance of the spherical model is indeed excellent, other kinds of interpolation, such as Cokriging and Compositional Kriging, may offer advantages in specific circumstances. Comparisons between these methods in identical conditions will help to pin down the best approach for a particular study area.

The model is highly accurate in modeling soil conditions with a MSE of 0.002084 found from cross-validation results. It easily outperforms other interpolation methods. Moreover, the spherical model is widely used for point Kriging because of its high accuracy and has always been a leader in soil property estimation. In this study, we further demonstrated that it can be used as a means of interpolating information obtained from sample points on the spatial variation size distribution of soil particles and proved empirically that such use will give good results.

The importance of selecting a good one of the various possible variogram models must not be underestimated as it has a direct bearing on accuracy in spatial interpolation [30] confirmed that variogram parameters are significantly related to the performance of the interpolation model. The spherical model, which best represents smooth spatial continuity, performed better than Exponential and Gaussian models in different geospatial cases.

Kriging simulation techniques work to generate multiple realizations of soil particle distribution consistent with the probability distribution. This deepens our understanding of spatial structures in soil management and land-use planning. Kriging-based estimates integrated with remote sensing data and machine learning approaches could further improve performance.

Recent advances in mathematical modeling have accentuated the importance of geophysical fluid flow dynamics in environmental modeling. For instance, by introducing the deep-water stratification effects into land surface processes, it would render Kriging simulations more precise in their predictions of soil particle distribution.

Future research should investigate the applicability of Kriging simulation models to various environmental conditions. The combination of hybrid modeling methods will no doubt greatly increase the accuracy of soil character predictions in different landscapes.

The result of validation for different models according to spherical model, Exponential model, and Gaussian model shows that the spherical model reaches the best results for soil particle distribution spatial patterns. Choosing an appropriate variogram model with validation results is key to improving accuracy in interpolation and spatial mapping.

Not only does adding other spatial modeling techniques improve the models based on Kriging, but they also offer further understanding of its underlying principles. For example, Geographically Weighted Ordinary Logistic Regression (GWOLR) can be combined with Kriging for finding an optimal soil particle size distribution [42] In this way, if we combine GWOLR with Kriging models, local variability capture is improved.

In addition, integrating cluster fast double bootstrap methods into random effect spatial models is useful in obtaining robustness and prediction precision from an array of geostatistical applications. The result of applying these techniques shows that as soil-classifying information becomes more sophisticated after training, a more efficient product is produced by using a professional platform and more photosynthesis coordination. When validating, although the performance of the spherical model was satisfactory, possible bias may still be introduced by the limited data basis for assumptions. Uneven sample distribution breeds interpolative errors, and this is especially concerning in Kriging predictions.

Deshmukh and Aher [43] showed that with increased sample density, the accuracy of extrapolation is heightened because more subtle patterns can be graphed. Therefore, it is a good idea to increase sample points and locate them carefully.

Further research should consider adaptive sampling strategies that adjust sample density on the basis of preliminary variogram analysis. Integrating remote sensing data and geostatistical simulation results with Kriging methods can fill in gaps left by sparsely sampled regions, improving the quality of soil particle distribution models. Sample representation should be optimized while simultaneously exploring external data sources and advanced geostatistical techniques.

Another consideration is that Kriging is based upon the assumption of stationarity—i.e., that soil particle distribution remains the same over a given scale. However, real-world factors such as hydrological changes and human activities can change soil distribution, so this is an assumption [44]. One more critical factor here is variogram modeling accuracy—poor predictor fitting strongly affects spatial predictions. And, in Kriging estimates on the whole, if spatial dependence deteriorates, it will seem less likely that interpolation should speak with more reliability.

Ngabu et al. [45] showed that adopting a cluster fast double bootstrap method combined with random effect spatial modeling yields statistically optimized geostatistical predictions. Similarly, Wang et al. [40] emphasized that robust variogram-estimation methods enhance the accuracy of spatial prediction. Therefore, total refinement through automated fitting algorithms that make optimization possible and cross-validation approaches is needed.

5. CONCLUSIONS

This paper reports an investigation on the distribution of soil particle size in Kalikonto Watershed (DAS) in Batu, Malang, using the Kriging method based on an experimental variogram. The research results include variogram parameters, the accuracy of the Kriging model prediction of soil properties, and its practical applications in agriculture and environmental management.

The analysis results showed that the spherical model is the best choice to portray the spatial distribution of soil particle size in the study area. With variogram parameters of Psill (68.9528), Range (4890.991), and Nugget (17.551), this study provides a clearer insight into the soil property variations in the region. The observed nugget effect reflects minor variations on a micro-scale, which might be due to measurement errors or natural differences in soil composition. With a range of 4.89 km, it suggests that there exist spatial relationships between measurement points up to this distance, and the reliability of forecasts by the Kriging method is thereby an important factor.

The Kriging model that was developed demonstrated a highly precise soil particle size forecast map. The results of cross-validation show that its error rate is very low (MSE = 0.002084), therefore meaning its predictions can effectively represent real soil conditions. Compared with exponential and Gaussian models, the spherical model performed better according to validation results.

The results of this study have wide practical benefits, especially in agricultural management and environmental conservation. The prediction map generated can help with determining where measures are needed, in particular for erosion control or even just in parts that need tougher treatment through soil management plans. Also, the data can be used for both the optimal combinations of fertilizers and strategies to conserve soil in those areas of high soil texture variability.

Nevertheless, in order to gain a more comprehensive understanding, this study needs comparison with other studies to determine whether the findings are specific only to unique factors within this larger general trend. Additional research might also be directed towards alternative methods, such as Compositional Kriging or Cokriging, which may be more effective under certain data conditions. Increasing the number of measurement points in areas with high variability could also help reduce uncertainty and raise forecast accuracy.

In sum, this study indicates the importance of careful selection of variogram model in the Kriging method in order to improve the accuracy of simulations of soil texture in space. These findings are an important reference for engineering, agricultural planning, as well as resource and environmental management.

ACKNOWLEDGMENT

We would like to thank Universitas Brawijaya for its support for this research. This research is an internal research grant from Universitas Brawijaya, namely the Superior Research Grant.

REFERENCES

[1] Ding, W., Huang, C. (2017). Effects of soil surface roughness on interrill erosion processes and sediment particle size distribution. Geomorphology, 295: 801-810. https://doi.org/10.1016/j.geomorph.2017.08.033

[2] Koiter, A.J., Owens, P.N., Petticrew, E.L., Lobb, D.A. (2017). The role of soil surface properties on the particle size and carbon selectivity of interrill erosion in agricultural landscapes. Catena, 153: 194-206. https://doi.org/10.1016/j.catena.2017.01.024

[3] Chen, Y., Liang, W., Li, Y., Wu, Y., Chen, Y., Xiao, W., Zhao, L., Zhang, J., Li, H. (2019). Modification, application and reaction mechanisms of nano-sized iron sulfide particles for pollutant removal from soil and water: A review. Chemical Engineering Journal, 362: 144-159. https://doi.org/10.1016/j.cej.2018.12.175

[4] Xu, H., Liu, K., Zhang, W., Rui, Y., Zhang, J., Wu, L., Colinet, G., Huang, Q., Chen, X., Xu, M. (2020). Long-term fertilization and intensive cropping enhance carbon and nitrogen accumulated in soil clay-sized particles of red soil in South China. Journal of Soils and Sediments, 20: 1824-1833. https://doi.org/10.1007/s11368-019-02544-8

[5] Lahive, E., Walton, A., Horton, A.A., Spurgeon, D.J., Svendsen, C. (2019). Microplastic particles reduce reproduction in the terrestrial worm Enchytraeus crypticus in a soil exposure. Environmental Pollution, 255: 113174. https://doi.org/10.1016/j.envpol.2019.113174

[6] Biswas, A., Biswas, A. (2024). Geostatistics in soil science: A comprehensive review on past, present and future perspectives. Journal of the Indian Society of Soil Science, 72(1): 1-22. http://doi.org/10.5958/0974-0228.2024.00017.1

[7] Keesari, T., Ramakumar, K.L., Chidambaram, S., Pethperumal, S., Thilagavathi, R. (2016). Understanding the hydrochemical behavior of groundwater and its suitability for drinking and agricultural purposes in Pondicherry area, South India – A step towards sustainable development. Groundwater for Sustainable Development, 2-3: 143-153. https://doi.org/10.1016/j.gsd.2016.08.001

[8] Kim, K.M., Lim, J., Choi, S.E., Cho, N., Seo, M., Lee, S., Woo, H., Lee, J., Lee, C., Lee, J. (2024). Advancement and applications of forest remote sensing

in Korea: Past, present, and future perspectives. Korean Journal of Remote Sensing, 40(5): 783-812. https://doi.org/10.7780/kjrs.2024.40.5.2.8
[9] Criado, M., Martínez-Graña, A., Santos-Francés, F., Merchán, L. (2021). Improving the management of a semi-arid agricultural ecosystem through digital mapping of soil properties: The case of Salamanca (Spain). Agronomy, 11(6): 1189. https://doi.org/10.3390/agronomy11061189
[10] Zhang, H., Wang, C., Chen, Z., Kang, Q., Xu, X., Gao, T. (2022). Performance comparison of different particle size distribution models in the prediction of soil particle size characteristics. Land, 11(11): 2068. https://doi.org/10.3390/land11112068
[11] Liu, Z., Dugan, B., Masiello, C.A., Gonnermann, H.M. (2017). Biochar particle size, shape, and porosity act together to influence soil water properties. PloS One, 12(6): e0179079. https://doi.org/10.1371/journal.pone.0179079
[12] Xue, W., Huang, D., Zeng, G., Wan, J., Cheng, M., Zhang, C., Hu, C., Li, J. (2018). Performance and toxicity assessment of nanoscale zero valent iron particles in the remediation of contaminated soil: A review. Chemosphere, 210: 1145-1156. https://doi.org/10.1016/j.chemosphere.2018.07.118
[13] Matus, F.J. (2021). Fine silt and clay content is the main factor defining maximal C and N accumulations in soils: A meta-analysis. Scientific Reports, 11(1): 6438. https://doi.org/10.1038/s41598-021-84821-6
[14] Jamaly, M., Kleissl, J. (2017). Spatiotemporal interpolation and forecast of irradiance data using Kriging. Solar Energy, 158: 407-423. https://doi.org/10.1016/j.solener.2017.09.057
[15] Wu, R., Xia, J., Chen, K., Chen, J., Liu, Q., Jin, W. (2023). Spatiotemporal interpolation of surface chloride content for marine RC structures based on non-uniform spatiotemporal Kriging interpolation method. Structural Safety, 103: 102329. https://doi.org/10.1016/j.strusafe.2023.102329
[16] Varatharajan, R., Vasanth, K., Gunasekaran, M., Priyan, M., Gao, X.Z. (2018). An adaptive decision based Kriging interpolation algorithm for the removal of high density salt and pepper noise in images. Computers & Electrical Engineering, 70: 447-461. https://doi.org/10.1016/j.compeleceng.2017.05.035
[17] Lebrenz, H., Bárdossy, A. (2019). Geostatistical interpolation by quantile Kriging. Hydrology and Earth System Sciences, 23(3): 1633-1648. https://doi.org/10.5194/hess-23-1633-2019
[18] Meng, J. (2021). Raster data projection transformation based-on Kriging interpolation approximate grid algorithm. Alexandria Engineering Journal, 60(2): 2013-2019. https://doi.org/10.1016/j.aej.2020.12.006
[19] Kerry, K.E., Hawick, K.A. (1998). Kriging interpolation on high-performance computers. In High-Performance Computing and Networking: International Conference and Exhibition Amsterdam, The Netherlands, pp. 429-438. https://doi.org/10.1007/BFb0037170
[20] Stein, M.L. (1999). Interpolation of Spatial Data: Some Theory for Kriging. Springer Science & Business Media.
[21] Bárdossy, A. (1997). Introduction to geostatistics. Institute of Hydraulic Engineering, University of Stuttgart, pp. 28-32.
[22] Oliver, M.A., Webster, R. (1990). Kriging: A method of interpolation for geographical information systems. International Journal of Geographical Information System, 4(3): 313-332. https://doi.org/10.1080/02693799008941549
[23] Trochu, F. (1993). A contouring program based on dual Kriging interpolation. Engineering with Computers, 9: 160-177. https://doi.org/10.1007/bf01206346
[24] Burgess, T.M., Webster, R. (1980). Optimal interpolation and isarithmic mapping of soil properties: I The semi-variogram and punctual Kriging. Journal of Soil Science, 31(2): 315-331. https://doi.org/10.1111/j.1365-2389.1980.tb02084.x
[25] Bostan, P. (2017). Basic Kriging methods in geostatistics. Yuzuncu Yıl University Journal of Agricultural Sciences, 27(1): 10-20. https://doi.org/10.29133/yyutbd.305093
[26] Zimmerman, D.L., Zimmerman, M.B. (1991). A comparison of spatial semivariogram estimators and corresponding ordinary Kriging predictors. Technometrics, 33(1): 77-91. https://doi.org/10.1080/00401706.1991.10484771
[27] Iriany, A., Ngabu, W., Arianto, D., Putra, A. (2023). Classification of stunting using geographically weighted regression-Kriging case study: Stunting in East Java. BAREKENG: Jurnal Ilmu Matematika Dan Terapan, 17(1): 495-504. https://doi.org/10.30598/barekengvol17iss1pp0495-0504
[28] Wang, Z., Shi, W. (2017). Mapping soil particle-size fractions: A comparison of compositional Kriging and log-ratio Kriging. Journal of Hydrology, 546: 526-541. https://doi.org/10.1016/j.jhydrol.2017.01.029
[29] Keshavarzi, A., Tuffour, H.O., Brevik, E.C., Ertunç, G. (2021). Spatial variability of soil mineral fractions and bulk density in Northern Ireland: Assessing the influence of topography using different interpolation methods and fractal analysis. Catena, 207: 105646. https://doi.org/10.1016/j.catena.2021.105646
[30] Li, J., Wan, H., Shang, S. (2020). Comparison of interpolation methods for mapping layered soil particle-size fractions and texture in an arid oasis. Catena, 190: 104514. https://doi.org/10.1016/j.catena.2020.104514
[31] Wang, Z., Shi, W. (2018). Robust variogram estimation combined with isometric log-ratio transformation for improved accuracy of soil particle-size fraction mapping. Geoderma, 324: 56-66. https://doi.org/10.1016/j.geoderma.2018.03.007
[32] Shtiliyanova, A., Bellocchi, G., Borras, D., Eza, U., Martin, R., Carrère, P. (2017). Kriging-based approach to predict missing air temperature data. Computers and Electronics in Agriculture, 142: 440-449. https://doi.org/10.1016/j.compag.2017.09.033
[33] Lu, P., Xu, Z., Chen, Y., Zhou, Y. (2020). Prediction method of bridge static load test results based on Kriging model. Engineering Structures, 214: 110641. https://doi.org/10.1016/j.engstruct.2020.110641
[34] Gribov, A., Krivoruchko, K. (2020). Empirical Bayesian Kriging implementation and usage. Science of the Total Environment, 722: 137290. https://doi.org/10.1016/j.scitotenv.2020.137290
[35] Yang, D. (2018). Spatial prediction using Kriging ensemble. Solar Energy, 171: 977-982. https://doi.org/10.1016/j.solener.2018.06.105
[36] Van Beers, W.C.M., Kleijnen, J.P.C. (2004). Kriging

interpolation in simulation: A survey. Proceedings of the 2004 Winter Simulation Conference, 2004(1). https://doi.org/10.1109/WSC.2004.1371308
[37] Van Beers, W.C.M., Kleijnen, J.P.C. (2003). Kriging for interpolation in random simulation. Journal of the Operational Research Society, 54: 255-262. https://doi.org/10.1057/palgrave.jors.2601492
[38] Puppo, L., Pedroni, N., Bersano, A., Di Maio, F., Bertani, C., Zio, E. (2021). Failure identification in a nuclear passive safety system by Monte Carlo simulation with adaptive Kriging. Nuclear Engineering and Design, 380: 111308. https://doi.org/10.1016/j.nucengdes.2021.111308
[39] Liu, L.L., Cheng, Y.M. (2018). System reliability analysis of soil slopes using an advanced Kriging metamodel and quasi–Monte Carlo simulation. International Journal of Geomechanics, 18(8): 6018019. https://doi.org/10.1061/(ASCE)GM.1943-5622.0001209
[40] Wang, Z., Shi, W., Zhou, W., Li, X., Yue, T. (2020). Comparison of additive and isometric log-ratio transformations combined with machine learning and regression Kriging models for mapping soil particle size fractions. Geoderma, 365: 114214. https://doi.org/10.1016/j.geoderma.2020.114214
[41] Sun, X.L., Wu, Y.J., Wang, H.L., Zhao, Y.G., Zhang, G.L. (2014). Mapping soil particle size fractions using compositional Kriging, cokriging and additive log-ratio cokriging in two case studies. Mathematical Geosciences, 46: 429–443. https://doi.org/10.1007/s11004-013-9512-z
[42] Pramoedyo, H., Ngabu, W., Riza, S., Iriany, A. (2024). Spatial analysis using geographically weighted ordinary logistic regression (GWOLR) method for prediction of particle-size fraction in soil surface. IOP Conference Series: Earth and Environmental Science, 1299(1): 12005. https://doi.org/10.1088/1755-1315/1299/1/012005
[43] Deshmukh, K.K., Aher, S.P. (2014). Particle size analysis of soils and its interpolation using GIS technique from Sangamner area, Maharashtra, India. International Research Journal of Environment Sciences, 3(10): 32-37.
[44] Lark, R.M., Bishop, T.F.A. (2007). Cokriging particle size fractions of the soil. European Journal of Soil Science, 58(3): 763-774. https://doi.org/10.1111/j.1365-2389.2006.00866.x
[45] Ngabu, W., Fitriani, R., Pramoedyo, H., Astuti, A.B. (2023). Cluster fast double bootstrap approach with random effect spatial modeling. BAREKENG: Jurnal Ilmu Matematika Dan Terapan, 17(2): 945-954. https://doi.org/10.30598/barekengvol17iss2pp0945-0954